ARTICLE
Journal of Cellular Biochemistry 112:2392–2402 (2011)

Journal of Cellular Biochemistry

Axin1 Expression Facilitates Cell Death Induced by Aurora Kinase Inhibition Through PARP Activation

Eun-Jin Choi,[1] Shi-Mun Kim,[1] Ki-Joon Song,[1] Jae-Myun Lee,[2] and Sun-Ho Kee[1*]

[1]*Laboratory of Cell Biology, Department of Microbiology and Bank for Pathogenic Virus, College of Medicine, Korea University, Seoul 136-705, Korea*

[2]*Department of Microbiology, College of Medicine, Yonsei University, Seoul 130-743, Korea*

ABSTRACT

Axin, a negative regulator of Wnt signaling, participates in apoptosis, and Axin1 localizes to centrosomes and mitotic spindles, which requires Aurora kinase activity. In this study, Aurora inhibition of Axin1-expressing cells (L-Axin) produced polyploid cells, which died within 48 h posttreatment, whereas Axin2-expressing cells (L-Axin2) survived the same period. These cell death events showed apoptotic signs, such as chromatin condensation and increased sub-G1 populations, as well as cell membrane rupture. Further analysis showed that Aurora kinase inhibitor (AKI) treatment of L-Axin cells induced poly(ADP-ribose) polymerase (PARP) activation, which increased the poly(ADP-ribosyl)ation of cellular proteins and reduced cellular ATP content. PARP inhibition reduced a proportion of dead cells, suggesting PARP involvement in AKI-induced cell death. Also, AKI treatment of L-Axin cells induced mitochondrial apoptosis-inducing factor (AIF) release, but not mitochondrial cytochrome *c* release or caspase-3 activation. Knockdown of AIF attenuated AKI-induced cell death in L-Axin cells. Thus, our results suggest that Axin1 expression renders L929 cells sensitive to Aurora inhibition-induced cell death in a PARP- and AIF-dependent manner. J. Cell. Biochem. 112: 2392–2402, 2011.

KEY WORDS: AXIN; AURORA KINASE; CELL DEATH; PARP; AIF

Aurora kinases, which regulate mitotic progression in various organisms, are evolutionarily conserved [Li and Li, 2006]. Aurora A and B are over-expressed in a wide range of human cancers, including colorectal, lung, breast, gastric, ovarian, and pancreatic cancers [Tong et al., 2004; Tarnawski et al., 2005; Vischioni et al., 2006; Fu et al., 2007]. Over-expression of Aurora A leads to aberrant mitosis and transforms mammary epithelial and embryonic fibroblast cells to genetically unstable aneuploid cells with multiple centrosomes [Zhang et al., 2004]. These observations have led to efforts to develop Aurora kinase inhibitors (AKIs) for use in cancer treatment. The inhibition of Aurora A activity induces abnormal spindle formation or chromosomal misalignment, whereas Aurora B inhibition induces cytokinesis failure [Ditchfield et al., 2003; Yang et al., 2005; Hoar et al., 2007]. When both Aurora A and B are chemically inhibited, the most prominent phenotypic change is polyploid cell generation, as Aurora A-induced mitotic arrest is transient [Yang et al., 2005]. In addition, AKI has shown antitumor effects via apoptosis induction [Curry et al., 2009; Li et al., 2010]. The mechanism of AKI-induced apoptosis appears complicated. Some studies have proposed a p53-dependent mechanism [Kojima et al., 2008; Dreier et al., 2009], whereas others have demonstrated that AKI-induced apoptosis requires a compromised p53-dependent postmitotic checkpoint [Ditchfield et al., 2003; Gizatullin et al., 2006].

Axin is a major negative regulator of canonical Wnt signaling, which regulates cell proliferation and cell fate determination [Salahshor and Woodgett, 2005]. The scaffolding activity of Axin leads to the formation of a complex consisting of β-catenin, adenomatous polyposis coli (APC), and glycogen synthase kinase 3β (GSK3β), which down-regulates Wnt signaling activity by destabilizing the cytoplasmic β-catenin. In addition to this canonical Wnt signaling, Axin interaction with numerous cellular proteins has been implicated in stress-activated protein kinase (SAPK) signaling, transforming growth factor β (TGFβ) signaling [Salahshor and Woodgett, 2005], and Dishevelled (Dsh)-mediated noncanonical Wnt signaling [Gao and Chen, 2010].

Axin1 appears to participate in the induction of cell death. Axin1 over-expression, which can induce apoptosis in CHO cells, seems to

Additional supporting information may be found in the online version of this article.

Eun-Jin Choi and Shi-Mun Kim contributed equally to this work.

Grant sponsor: KOSEF; Grant numbers: 2009-0080582, R21-2005-000-10017-02007.

*Correspondence to: Sun-Ho Kee, Laboratory of Cell Biology, Department of Microbiology and Bank for Pathogenic Virus, College of Medicine, Korea University, Seoul 136-705, Korea. E-mail: keesh@korea.ac.kr

Received 25 August 2010; Accepted 19 April 2011 • DOI 10.1002/jcb.23162 • © 2011 Wiley-Liss, Inc.
Published online 25 April 2011 in Wiley Online Library (wileyonlinelibrary.com).

be mediated by JNK signaling, as deletion of the MEKK1 interacting domain attenuates the apoptotic effect [Neo et al., 2000]. In another line of evidence, Axin1 appears to be involved in a DNA damage-induced, Daxx-mediated cell death mechanism [Li et al., 2007, 2009], in which the role of Axin1 is particularly emphasized, as Axin1 regulates p53 activity via its competitive binding capacity to Pirh2 or Tip60 [Li et al., 2009].

Axin1 and its homolog, Axin2, have high sequence similarity at the nucleotide level and appear to be functionally similar. When over-expressed in cultured cells, both proteins are able to reduce the level of β-catenin and the expression of Wnt target genes [Behrens et al., 1998; Sakanaka et al., 1998; Chia and Costantini, 2005]. When expressed in frog embryos, both Axin1 and Axin2 inhibit the development of dorsal structures [Zeng et al., 1997; Itoh et al., 1998; Yamamoto et al., 1998; Chia and Costantini, 2005]. However, they are not fully redundant in vivo, as Axin2 is unable to compensate completely for the absence of Axin1 in *Axin*-null embryos [Zeng et al., 1997]. Moreover, whereas Axin1 is expressed ubiquitously during embryogenesis, Axin2 is expressed in a restricted pattern [Zeng et al., 1997]. Axin2 localizes along microtubules and binds to polo-like kinase 1, and up-regulation of Axin2 leads to chromosomal instability [Hadjihannas et al., 2006]. In contrast, others demonstrated that both Axin1 and Axin2 localized to centrosomes and to mitotic spindles [Fumoto et al., 2009; Kim et al., 2009]. In centrosomes, Axin1, but not Axin2, formed a complex with γ-tubulin and was involved in microtubule nucleation [Fumoto et al., 2009]. These results suggest different functions of Axin1 and Axin2, possibly due to the cellular context. Previously, we described that centrosomal localization of Axin was suppressed by siRNA specific for Aurora kinase and by AKI [Kim et al., 2009]. Considering that Aurora kinase inhibition is implicated as an anticancer strategy, we analyzed the influences of Axin1 and Axin2 on AKI-induced cytotoxicity.

In this study, we observed that Axin1 expression rendered L929 cells more sensitive to AKI-induced cell death than Axin2. Also, AKI treatment of L929 cells over-expressing Axin1 (L-Axin) induced poly(ADP-ribose) polymerase (PARP) activation, which in turn reduced cellular ATP content and led to the release of mitochondrial apoptosis-inducing factor (AIF).

MATERIALS AND METHODS

CELLS, CHEMICALS, AND ANTIBODIES

L929 cells were maintained in Dulbecco's modified Eagle's medium supplemented with 10% (v/v) fetal bovine serum (Cambrex, Madrid, Spain). L929 cells that expressed green fluorescence protein (GFP) and ectopic Axin1 or Axin2 simultaneously in a doxycyclin-inducible manner (L-Axin or L-Axin2) were established as described previously [Jeon et al., 2007; Kim et al., 2009]. Control cells were established by the transfection of an empty vector (L-EV). Aurora kinase inhibitor (AKI), caspase inhibitor (z-VAD-FMK), PARP inhibitor (INH_2BP; 5-iodo-6-amino-1,2-benzopyrone), and staurosporine were purchased from Calbiochem (La Jolla, CA) and used at working concentrations of 17, 100, 50, and 0.5 μM, respectively. The following antibodies were used: cytochrome *c*, apoptosis-inducing factor (AIF), PARP (BD Pharmingen, San Diego, CA), active caspase-3 (Cell Signaling Technology, Beverly, MA), and GAPDH (Santa Cruz Biotechnology, Santa Cruz, CA).

TRANSFECTION

Cells were grown to 40–60% confluency on round coverslips and transfected with 100 pmol siRNA (control-scrambled; Bioneer Corporation, Daejeon, Korea) using Lipofectamine™ (Invitrogen, Carlsbad, CA). The sequences of the siRNA mouse PARP-1 were 5′-UAAAGAAGCUGACGGUGAA-3′ (siPARP1a) and 5′-CAAA-GUAUCCCAAGAAGUU-3′ (siPARP1b). The sequences of the siRNA mouse AIF were 5′-AAG AGA AAC AGA GAA GAG CCA-3′ (siAIF-1) and 5′ GCAUGCUUCUAUGAUAUAA-3′ (siAIF-2).

FACS ANALYSIS

Fluorescence-activated cell sorting (FACS) analysis of propidium iodide-stained DNA contents was conducted as previously described [Kim et al., 2009]. To characterize the mode of cell death, the Annexin V-PE apoptosis detection kit was used according to the manufacturer's instructions (BD Pharmingen). Briefly, cells treated with AKI were harvested and suspended in binding buffer (10 mM HEPES, 140 mM NaCl, 2.5 mM $CaCl_2$). Then, 1×10^5 cells were stained with Annexin V-PE or 7-amino-actinomycin D (7-AAD). To measure the mitochondrial membrane potential, cells (1×10^6) were prepared and incubated in phosphate-buffered saline (PBS, pH 7.2) containing 50 nM tetramethylrhodamine ethyl ester (TMRE; Invitrogen) for 20 min at 37°C in a 5% CO_2 incubator. After centrifuging, cell pellets were re-suspended in fresh PBS containing 50 nM TMRE. The fluorescence emitted from cells was measured via flow cytometry using a FACSCalibur™ Flow Cytometer (BD Biosciences) and analyzed using WinMDI 2.9 (Joseph Trotter, Scripps Research Institute, La Jolla, CA) software.

IMAGING

Immunofluorescence (IF) staining was performed as described previously [Kim et al., 2009]. For time-lapse imaging, L929 cells grown on 35-mm dishes were treated with AKI, and live images were taken at 6-min intervals beginning 10 h posttreatment using an Observer D1 phase-contrast microscope equipped with a CCD camera (Carl Zeiss, Oberkochen, Germany). For chromatin staining, Hoechst dye (200 ng/ml) was added to the culture medium 20 h after imaging began (i.e., 30 h posttreatment), and fluorescence images were taken for 1 h. Digital images were collected and processed using AxioVision software (Carl Zeiss). In some cases, fluorescence images were analyzed using confocal laser scanning microscopy (LSM510, Carl Zeiss).

TUNEL ASSAY

For the terminal deoxynucleotidyl transferase-mediated dUTP nick end labeling (TUNEL) assay, we used the Applied Science In Situ Cell Death Detection Kit (Roche, Penzberg, Germany) and performed the experiment according to the manufacturer's instructions. Briefly, 2×10^4 cells were grown on a 24-well plate and treated with the appropriate chemicals. Cells were rinsed with PBS (pH 7.2) three times and permeabilized with PBS containing 0.4% Triton X-100 for 40 min at 4°C. After washing with PBS three times, cells were incubated with TUNEL assay solution, including terminal deox-

ynucleotidyl transferase, for 1 h at 37°C. After washing with PBS three times, stained cells were analyzed via fluorescence microscopy (Axioscope; Carl Zeiss). Fluorescence images were captured with a digital camera (Roper Scientific, Trenton, NJ) and processed using MetaVue software (Universal Imaging Corporation, Downingtown, PA).

CELLULAR ATP MEASUREMENT

Intracellular ATP content was measured with a Luminescence ATP Detection Assay System (ATPlite, PerkinElmer, Inc., Waltham, MA) according to the manufacturer's instructions. Briefly, cells grown in a 96-well plate were treated with various chemicals and then lysed with mammalian cell lysis solution for 5 min at room temperature. Luminescence was measured after substrate addition.

CELL FRACTIONATION AND IMMUNOBLOT ANALYSIS

L929 cells were cultured on 100-mm dishes, suspended by scraping in a hypotonic solution (10 mM HEPES, pH 7.9; 10 mM KCl; 0.1 mM EDTA; 1 mM DTT; 0.5 mM PMSF), and incubated on ice for 15 min, after which NP-40 was added. The swelled cells were homogenized. The pellet was removed by centrifuging at 400 rpm for 5 min. To isolate the mitochondrial fraction, the supernatant was centrifuged at 13,000 rpm for 15 min. The resulting supernatant and pellet were used as the crude cytosolic and mitochondrial fraction, respectively.

RESULTS

AURORA KINASE INHIBITION FACILITATES CELL DEATH IN AXIN OVER-EXPRESSING CELLS

Previously, we reported that Axin, aided by Aurora kinase activity, localizes to mitotic spindles and centrosomes, and that Aurora kinase inhibition of Axin over-expressed cells alters the cytokinetic process [Kim et al., 2009]. To determine the fate of Axin over-expressed cells in the absence of Aurora kinase activity, L cells which express Axin1 or Axin2 (L-Axin or L-Axin2 cells, Fig. 1A) were treated with AKI for extended incubation period. Initial phase-contrast microscopic observation showed that rounded L-Axin cells increased 24 h after AKI treatment. At 48 h after AKI treatment, approximately 23% of L-Axin cells appeared to die, whereas most control L-EV and L-Axin2 cells remained viable (Fig. 1B,C). At 72 h, cell death of AKI-treated L-EV and L-Axin2 cells became apparent. In case of doxycyclin only treatment, all three cells including L-Axin cells remained viable for same period (Supplementary Fig. S1A), suggesting that cell death was due to AKI cytotoxicity. Furthermore, TUNEL assay revealed that a higher proportion of L-Axin cells underwent cell death than L-EV and L-Axin2 cells at

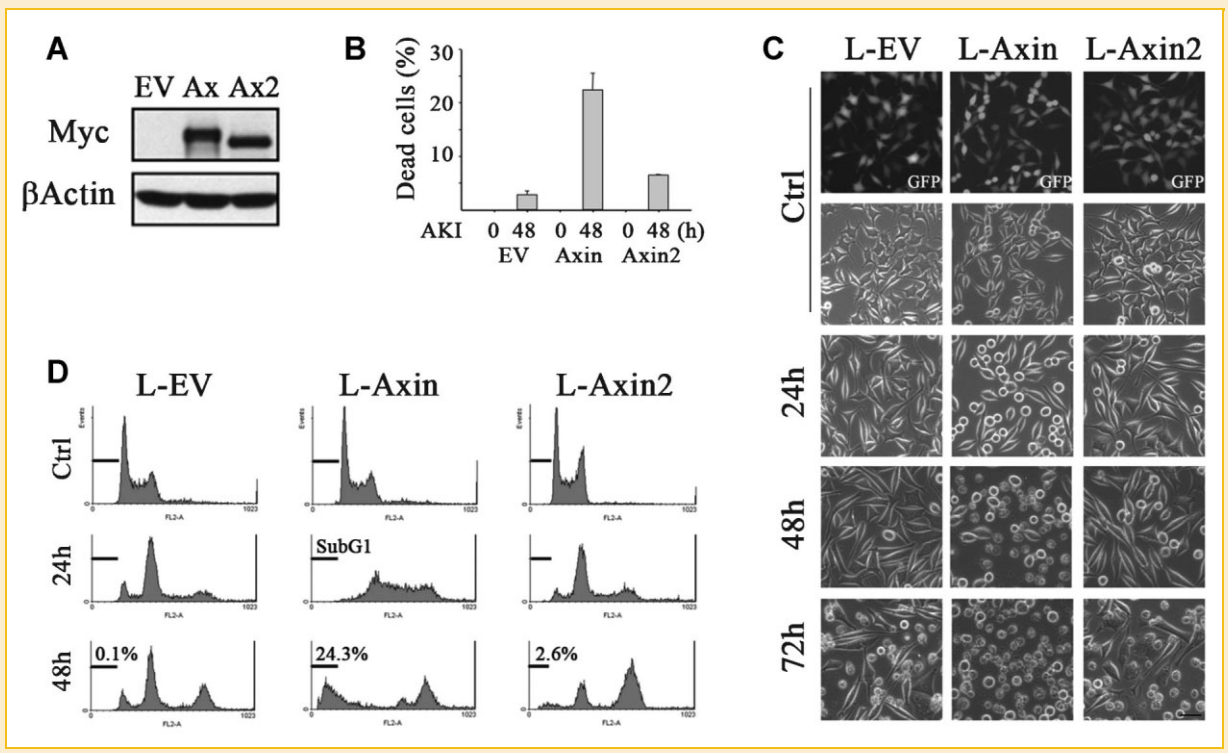

Fig. 1. Aurora inhibition induces cell rounding and cell death in L-Axin cells. A: L-cells which stably express Axin1 (L-Axin) or Axin2 (L-Axin2) as doxycyclin-inducible form were subjected to immunoblot analysis. Control cells which were transfected of vector only were also analyzed. Similar level of Axin1 and Axin2 expression was observed. B,C: L-EV, L-Axin and L-Axin2 cells were treated with doxycyclin and Aurora kinase inhibitor (AKI) and subjected to phase-contrast microscopic observation. Bar: 100 μm (C). Dead cells were quantitated by direct counting. The results of average values of three independent experiments (B). D: L-EV, L-Axin and L-Axin2 cells were treated with doxycyclin and Aurora kinase inhibitor (AKI) for 24 or 48 h and subjected to DNA analysis. Horizontal bars indicate area of subG1 population and percent proportions of subG1 population is also presented.

48 h after AKI treatment (Supplementary Fig. S1B). In addition, DNA analysis showed that AKI treatment generated polyploid cells in all three cell types at 24 h of AKI treatment. The sub-G1 proportion of L-Axin cells was elevated to about 24% at 48 h of AKI treatment, whereas L-EV and L-Axin2 cells showed only a slight increase (less than 3%; Fig. 1D). These results suggest that Axin1 over-expression facilitates AKI-induced cell death more efficiently than Axin2. To verify the effects of Axin2 on AKI-induced cell death, several cell lines that showed an increase in Axin2 expression were analyzed. Axin1 over-expression in naturally occurring cell lines is rarely observed. In Axin2-expressing cell lines such as SW480, AGS, and SNU 475 cells, only a small proportion of cells (i.e., 1–6%) died within 48 h of AKI treatment (Supplementary Fig. S2). These results might suggest that Axin2 over-expression does not influence AKI-mediated cytotoxicity.

AKI-INDUCED CELL DEATH IS ACCOMPANIED BY CELL MEMBRANE RUPTURE

To investigate the features of AKI-induced cell death, time-lapse analysis was performed. AKI-treated L-Axin cells showed abnormal mitosis with incomplete cytokinesis, resulting in polyploid cells. Further cultivation resulted in cells entering mitosis, at which stage they appeared to be arrested, followed by cell death with cell membrane rupture (Fig. 2A and Supplementary Movie 1). As most dead cells did not contain GFP, rupture of the cell membrane may release GFP. However, some cells with intact cell membranes (i.e., GFP expressing) were positively stained by TUNEL assay and contained micronuclei, suggesting that cell death was initiated before membrane rupture (Fig. 2B,C). Subsequent time-lapse analysis following Hoechst dye staining showed chromatin condensation in cells with GFP expression (Fig. 3A), which then underwent membrane rupture and GFP release. To confirm whether membrane rupture was the cause of cell death or an accompanying event, we performed FACS analysis using Annexin V and 7-AAD staining. Annexin V-staining appeared to increase slightly within the GFP-positive fraction (R3) in a time-dependent manner, whereas the proportion of double-negative cells (R2) remained low throughout the experiment (Fig. 3B). These results suggest that Annexin V-staining preceded membrane rupture (GFP release). The increase of 7-AAD and GFP double-positive cells was difficult to observe. Most GFP-negative cells showed weak 7-AAD staining (Fig. 3B), suggesting that 7-AAD did not efficiently stain these cells.

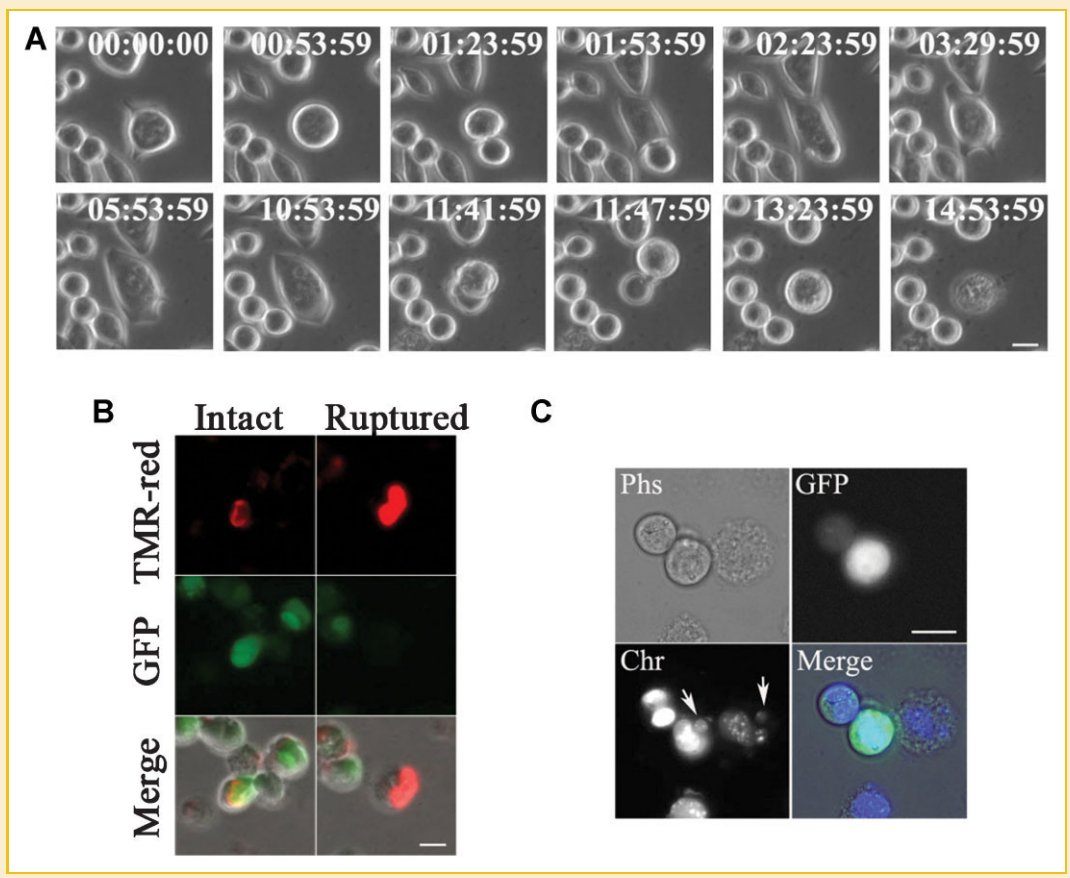

Fig. 2. Aurora inhibition of L-Axin cells induced cell membrane rupture. A: L-Axin cells were treated with doxycyclin and Aurora kinase inhibitor (AKI) and subjected to time-lapse imaging for 20 h beginning at 10 h posttreatment. Bar: 20 μm. B,C: AKI-treated L-Axin cells were TUNEL-stained (B) or stained with Hoescht dye (C). Cells with both intact and ruptured cell membranes (presence or absence of GFP, respectively) showed positive staining of TUNEL or micronuclei formation (arrows). Phs and Chr indicate phase contrast image and Chromatin staining by Hoescht dye. Bar: 20 μm.

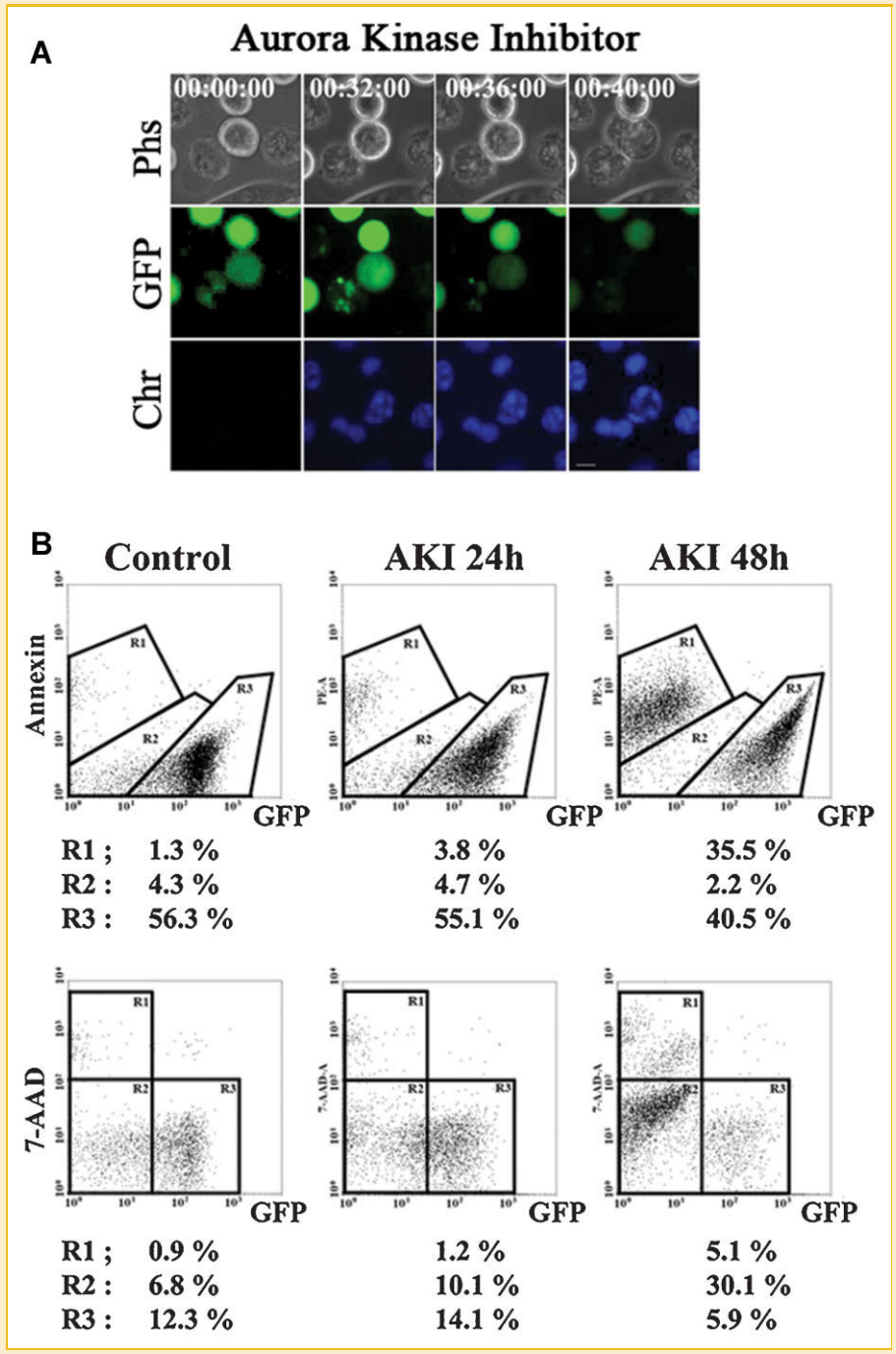

Fig. 3. Aurora kinase inhibitor (AKI) treatment of L-Axin cells induced chromatin condensation, followed by cell membrane rupture. A: L-Axin cells were treated with AKI in addition to doxycyclin, and then underwent time-lapse imaging, after which Hoescht dye was added to the medium; fluorescence and phase contrast images were taken for 1 h. The membranes of some cells with chromatin condensation were disintegrated. Bar: 10 μm. B: AKI-treated L-Axin cells were stained with Annexin V and 7-AAD and subjected to FACS analysis. Annexin V or 7-AAD stained cells were categorized into three fractions on the basis of GFP expression (*x*-axis): R1, Annexin- or 7-AAD-positive and GFP-negative cells; R2, double-negative cells; R3, GFP-positive cells. Result is a representative of two experiments.

All these results suggest that membrane rupture may accompany, rather than cause, cell death.

AKI INDUCES PARP ACTIVATION IN L-AXIN CELLS

Previous studies have shown that PARP is involved in either necrosis or apoptosis [Koh et al., 2005; Heeres and Hergenrother, 2007]. Among PARP family which is consisted of 17 members, PARP-1 is the prototypic and abundant nuclear protein. Cells devoid of PARP-1 are more sensitive to DNA damaging agents, such as alkylating drugs, suggesting a protective role from genotoxic stress. Conversely, in response to high levels of DNA damage, PARP-1 over-activation can lead to metabolic disturbance through

consumption of a substantial amount of cellular NAD^+, which results in necrotic cell death. Since AKI-induced cell death had necrotic cell death characteristics, such as cell membrane rupture, we examined PARP activity in AKI-treated L-Axin cells. PARP catalyses the transfer of the ADP-ribose moiety from NAD^+ to numerous proteins, including histones or PARP itself. Exposing L-Axin cells to AKI for 48 h induced a greater increase in poly(ADP-ribosyl)ation (PARylation) of cellular proteins than L-EV or L-Axin2 (Fig. 4A,B). Massive PARylation is known to result in rapid depletion of NAD^+ and ATP pools, which if not regulated, can lead to cellular dysfunction and cell death. A more profound reduction of cellular ATP levels was observed in AKI-treated L-Axin cells than other cells (Fig. 4C). This PARylation of proteins and ATP depletion were attenuated by PARP inhibitor in AKI-treated L-Axin cells (Fig. 5A,B and Supplementary Fig. S3), indicating that AKI treatment of L-Axin cells induced PARP activation to a greater extent than in other cells. Subsequent phase contrast observation showed that PARP inhibition reduced the dead cell proportion in AKI-treated L-Axin cells (Fig. 5C and Supplementary Fig. S4A). Similarly, TUNEL assay and DNA analysis demonstrated a reduction in cell death (Fig. 5D and Supplementary Fig. S4B). These results suggest that AKI-induced cell death may be mediated by PARP activation in L-Axin cells. Considering that PARP-1 is known to be the most abundant PARP in cells, specific knock-down of PARP-1 was performed using two PARP-1 specific siRNAs. Both siRNAs reduced PARP-1 expression efficiently in L-Axin cells (Fig. 6A) but reduction of AKI-induced PARylation of cellular proteins (Fig. 6A) and cell death (Fig. 6B) were not clear in comparison to effects of PARP inhibitor. These results suggest that activation of PARP-1 was not enough and other PARP isotype might be involved in AKI-induced cell death.

AKI INDUCES MITOCHONDRIAL AIF RELEASE IN L-AXIN CELLS

Over-activation of PARP induces metabolic disturbances that cause necrosis. Also, PARP activation is required for AIF-mediated apoptosis [Heeres and Hergenrother, 2007; Wang et al., 2009]. PARP activation induces the translocation of AIF from mitochondria to the nucleus where AIF interacts with cyclophilin A to form a degradosome that favors chromotinolysis. This apoptotic process is known to be caspase-independent. To explore the precise mechanism of AKI-induced cell death, involvement of caspase-3 was analyzed. Neither PARP cleavage nor caspase-3 activation was observed in AKI-treated L-Axin cells, although staurosporine (STS) induced both events (Fig. 7A). Furthermore, immunoblot analysis of cell lysates after subcellular fractionation also showed an absence of cytochrome *c* release, but an increase of cytoplasmic AIF was observed in AKI-treated L-Axin cells (Fig. 7B). For this assay, the nuclear fraction was omitted, as the AKI-induced cell death featured signs of mitotic catastrophe (Fig. 2C), and mitotic cells differ from interphase cells in subcellular compartmentation. Subsequent IF analysis revealed a speckled pattern of AIF staining in L-EV and L-Axin cells, but AKI-treated L-Axin cells were homogenous whereby only speckled patterns of cytochrome *c* were observed even in AKI-treated L-Axin cells (Fig. 7C,D). These results suggest that AIF was

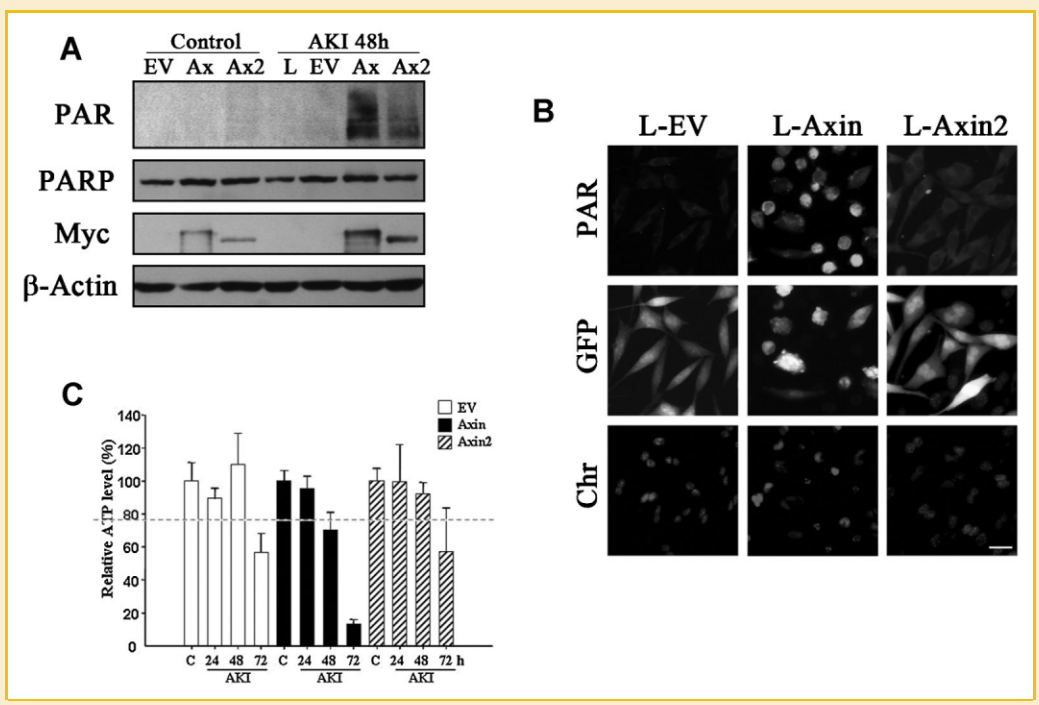

Fig. 4. Aurora inhibition induces PARP activation in L-Axin cells. A,B: L929 cells were treated with AKI in addition to doxycyclin, and then subjected to immunoblot (A) or immunofluorescence (B) analysis using anti-PAR antibody. EV indicates L-EV cell lysates. Ax and Ax2 indicate L-Axin and L-Axin2 cell lysates. Expression of ectopic Axin and amount of protein loading were verified using anti-Myc tag and anti-Actin antibody. Bar in (B): 100 μm. C: L929 cells were treated with AKI in addition to doxycyclin, and then subjected to cellular ATP measurement. This result is an average of three independent experiments. Horizontal dashed line indicates putative threshold of cellular ATP amount for cell viability.

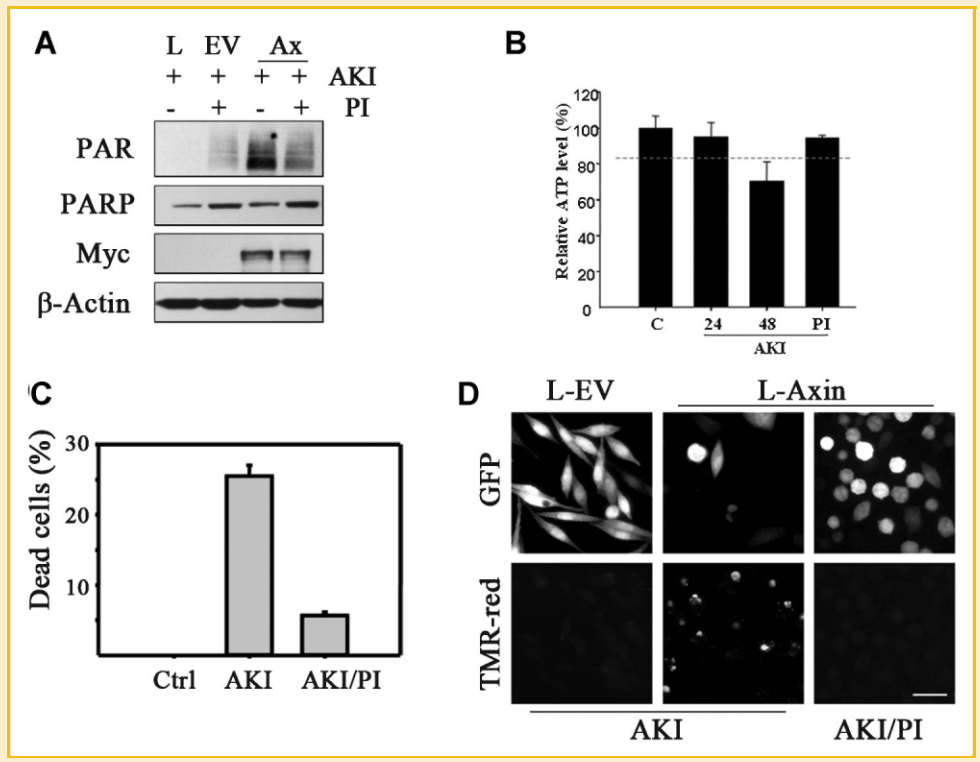

Fig. 5. PARP inhibition attenuates Aurora inhibition-induced cell death in L-Axin cells. A: L-EV and L-Axin cells were treated with AKI and PARP inhibitor (PI) and then subjected to immunoblot analysis using anti-PAR antibody. L indicates L929 cell lysates. EV and Ax indicate L-EV and L-Axin cell lysates, respectively. B: L-Axin cells were treated with AKI and PI together and then subjected to cellular ATP measurement. This result is an average of three experiments. C: L-Axin cells treated with AKI and PI were subjected to phase-contrast microscopic observation and dead cells were counted directly and quantitiated. This result is an average of three experiments. Representative phase-contrast of images were shown in supplementary Figure S4A. D: L-Axin cells treated with AKI and PI were subjected to TUNEL assay. A proportion of TUNEL positive cells was reduced by PARP inhibition. Bar: 100 μm.

released from mitochondria but not cytochrome *c*. To know if AIF release from mitochondria was required for AKI-induced cell death in L-Axin cells, an AIF knockdown experiment was performed using two kinds of AIF siRNA. Transfection of these AIF siRNAs reduced AIF expression (Fig. 8A and Supplementary Fig. S5B) and also reduced AKI-induced subG1 population in L-Axin cells (Fig. 8B). In addition, TUNEL-positive cells were reduced in AIF knockdown cells, compared to their level in scrambled siRNA transfected cells (Fig. 8C and Supplementary Fig. S5A,C). Moreover, inhibition of PARP activity blocked AIF release from mitochondria (Fig. 8D), which suggested that AKI treatment of L-Axin cells induced AIF-dependent cell death through PARP activation.

In conclusion, our results showed that Axin1 over-expression facilitates cell death induced by the inhibition of Aurora kinase activity, and that this effect was much weaker under the Axin2 over-expression condition. AKI treatment of L-Axin cells lead to PARP activation, which induced depletion of cellular ATP as well as released AIF from mitochondria. Eventually, these events produced cell death with mixed features of necrosis and apoptosis.

DISCUSSION

Axin1 has been reported to be the concentration-limiting factor in regulating the efficiency of the β-catenin destruction complex and level of Wnt signaling activity [Salahshor and Woodgett, 2005]. Biochemical studies have shown that the intracellular concentration of Axin is approximately 1,000-fold less than that of β-catenin, and Wnt signaling promotes the degradation of Axin1 [Willert et al., 1999; Leung et al., 2002]. Axin2 is known to be a major transcription target of the β-catenin/TCF complex and Axin2 expression is higher than that of Axin1 in several colon cancer cell lines (see Supplementary Fig. 2). These observations suggest a negative feedback function of Axin2 for Wnt signaling activity. However, cell lines expressing Axin2 seem to retain high a level of Wnt signaling activity, as antagonizing Wnt signaling in SW480 cells in the absence of Wnt3a-stimulation showed further inhibition of Wnt-responsive luciferase reporter activity [Huang et al., 2009]. These observations suggested that Axin2 may have a less efficient concentration-limiting regulatory function for Wnt signaling than Axin1. In addition, subtle differences between Axin1 and Axin2 have been described. For example, centrosomal localization of Axin2 were differently observed in several laboratories. Hadjihannas et al. showed that only Axin2 localize to centrosome/mitotic spindles and play a role in generation of chromosomal instability. In contrast, other report described that Axin1, but not Axin2 plays a role in microtubule nucleation through complex formation with γ-tubulin [Fumoto et al., 2009], whereas Axin2 regulates centrosome cohesion through interaction with C-Nap1 [Hadjihan-

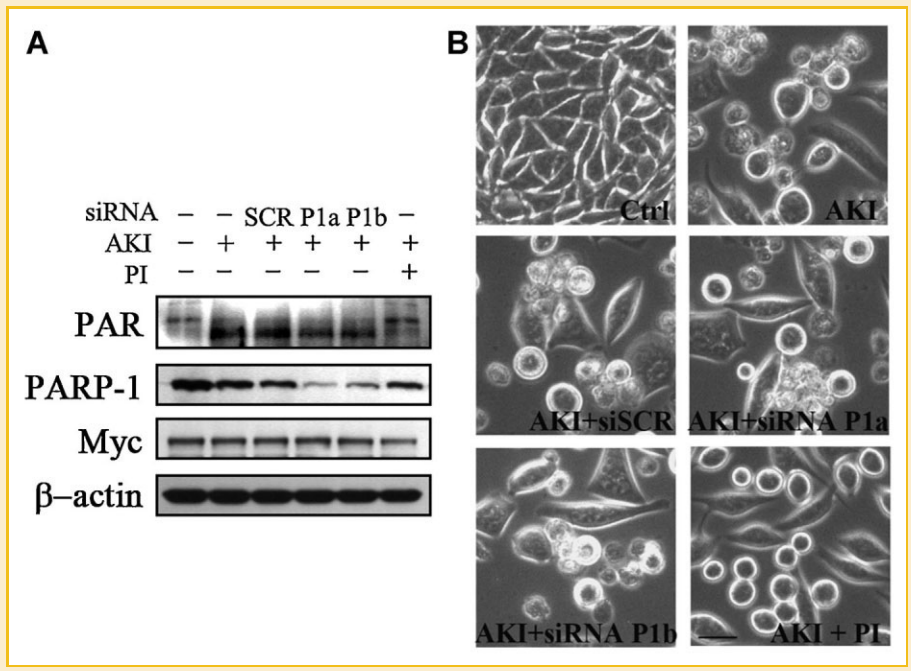

Fig. 6. Knockdown of PARP-1 does not suppress AKI-induced cell death. A: Two PARP-1 siRNAs were transfected to L-Axin cells and PARP-1 expression was monitored by immunoblot analysis. Both siRNAs transfection reduced PARP-1 expression but PARylation of cellular proteins was only slightly reduced. Expression of Myc-tagged Axin was not affected. P1a and P1b indicate PARP-1a and PARP-1b siRNA. B: L-Axin cell transfected by siRNAs PARP-1 were analyzed after AKI treatment for 48 h using phase contrast microscopy. Bar: 100 μm.

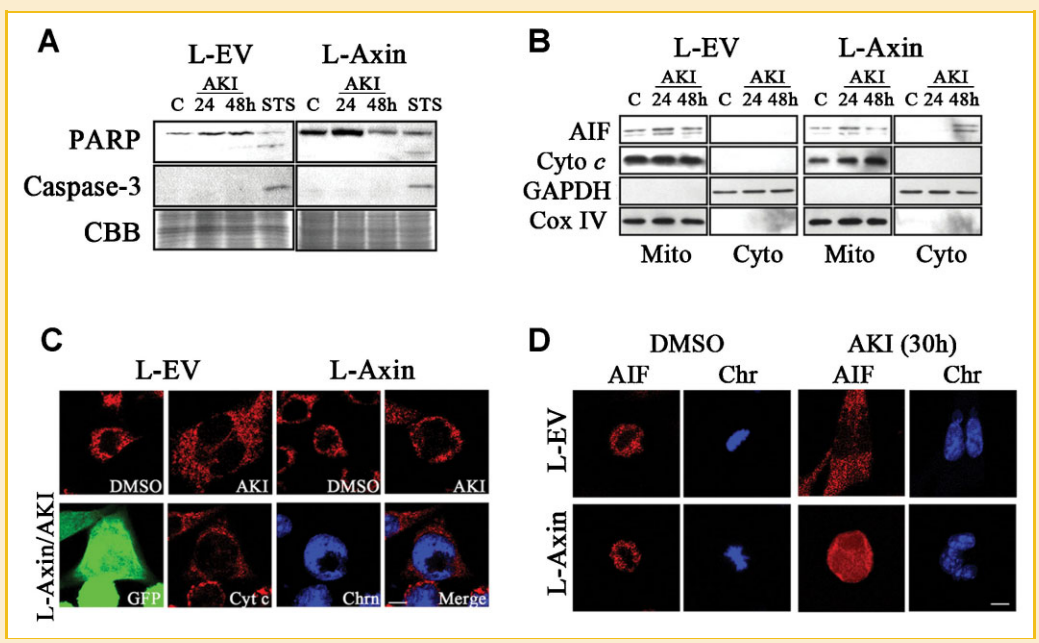

Fig. 7. Aurora inhibition induces mitochondrial AIF release but not mitochondrial cytochrome *c* release and caspase-3 activation. A: AKI or staurosporine (STS)-treated L-EV and L-Axin cells were subjected to immunoblot analysis using anti-PARP, anti-active caspase-3 antibodies. CBBS, Coomassie brilliant blue stain. B: L-EV or L-Axin cells were treated with AKI for 48 h, then subjected to subcellular fractionation. Immunoblot analysis using indicated antibodies was performed on organellar fractions, including the mitochondrial (Mito) and cytoplasmic (Cyto). Expression of cyclooxygenase IV (CoxIV) and GAPDH were used for verification of subcellular fractionation. C,D: AKI-treated L-EV or L-Axin cells were subjected to fluorescence labeling using anti-cytochrome *c* antibody (C) or anti-AIF antibody (D). Bar: 20 μm.

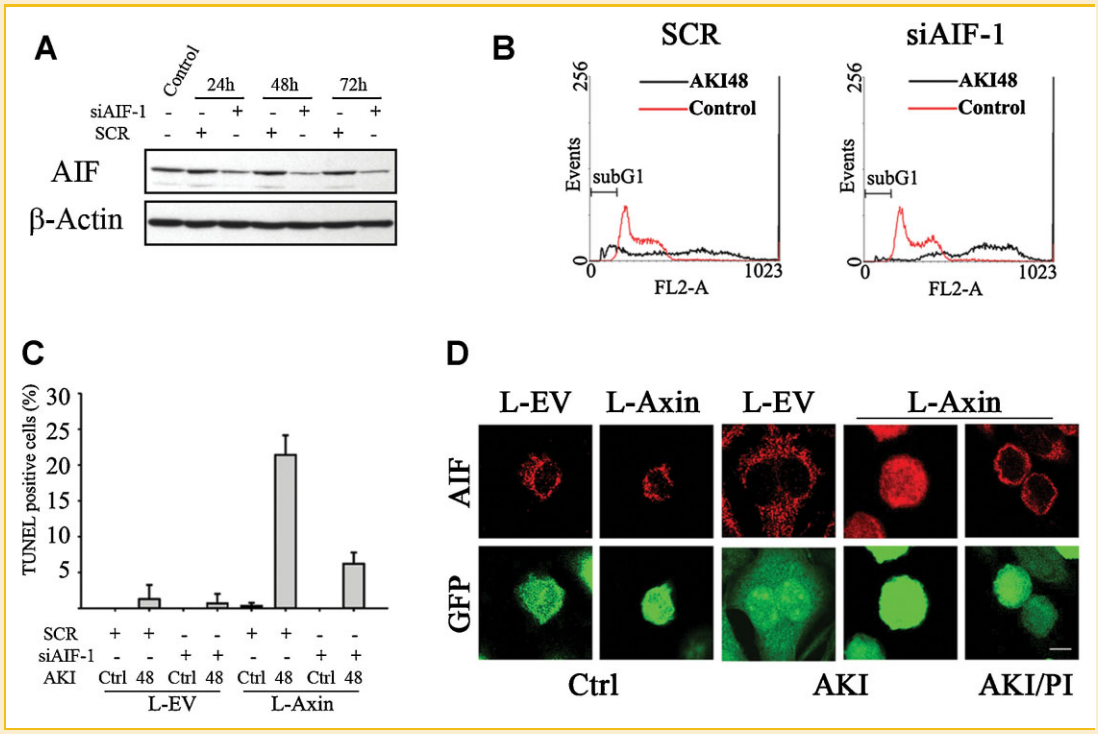

Fig. 8. Aurora kinase inhibitor (AKI) treatment induces AIF-mediated cell death. A: L929 cells were transfected with AIF siRNA-1 (siAIF-1), harvested after indicated incubation, and then subjected to imunoblot analysis using anti-AIF and anti-Actin antibody. B: L-Axin cells were transfected by scrambled siRNA (SCR) or siAIF-1 and cultivated 48 h, then subjected to DNA analysis. Transfection of siAIF-1 RNA increased polyploid cells without a subG1 population. C: L-Axin cells were transfected with SCR or siAIF-1 RNA, cultivated 48 h, and then subjected to TUNEL analysis. Triplicate TUNEL assay experiments were quantitated by direct counting. The proportion of TUNEL-positive cells is shown in the graph. Representative result of TUNEL images were shown in supplementary Figure S8A. D: L-EV and L-Axin cells were treated with PARP inhibitor (PI) together with AKI for 48 h and then subjected to fluorescence labeling using anti-AIF antibody. Bar: 20 μm.

nas et al., 2010]. These results suggested that Axin1 and Axin2 may conduct different functions according to different conditions. In our experimental condition, increased expression of Axin1 rendered cells sensitive to cell death stimulation by Aurora kinase inhibition, and these effects were less efficient in cells with Axin2 expression.

Generally, various cellular properties influence the mechanism of cell death. Aurora kinase inhibition produces different cell phenotypes in a variety of cell types, among which is the failure of proper chromosome segregation, coupled with the development of polyploidy in interphase cells [Ditchfield et al., 2003; Yang et al., 2005; Girdler et al., 2006]. Polyploid cells appear to be detected and eliminated at a p53-dependent postmitotic checkpoint [Margolis et al., 2003]. If the p53-dependent postmitotic checkpoint function was compromised, however, cells bypassed the postmitotic checkpoint and enhanced endoreduplication, leading to an accumulation of >4N DNA content, followed by cell death [Harrington et al., 2004; Gizatullin et al., 2006]. In our model, the AKI-induced cell death of L-Axin cells appeared to occur in a p53-dependent manner, as L929 cells have wild-type p53 alleles, and endoreduplication of L-Axin cells (>4N) was difficult to observe (Fig. 1C). These speculations were further supported by previous observations that Aurora A inhibition seems to increase sensitivity to apoptosis by stabilizing p53 via the inhibition of Mdm2-mediated p53 proteolysis [Katayama et al., 2004]. In addition, Axin1 can activate p53 in cooperation with Daxx and HIPK2, and the formation of a complex of Axin1, Pirh2, Tip60, HIPK2, and p53 may affect cell fate determinations [Li et al., 2007, 2009].

In terms of apoptosis, L929 cells show a distinct characteristic in the cell death mechanism. Although tumor necrosis factor (TNF) induces typical apoptotic death in many cell types, TNF caused non-apoptotic cell death in L929 cells [Vercammen et al., 1998a]. Treatment with caspase inhibitors, including zDEVD and zVAD, increased the sensitivity of L929 cells to TNF-mediated cell death [Vercammen et al., 1998a]. TNF-induced cell death of L929 cells may be mediated by PARP activation because TNF mediated PARP activation and PARP inhibitor suppressed TNF-induced cell death and the sensitizing effect of zVAD [Los et al., 2002]. Since Fas-transfected L929 cells showed rapid anti-Fas mAb-induced caspase-3-like protease activation, TNF-induced cell death of L929 cells is not resulted from null function of caspase-3 [Vercammen et al., 1998b]. On the consideration of these observations, AKI-induced phenotypes appeared similar to those of TNF-induced cell death of L929 cells. In fact, our similar experiments using HaCaT cells which were derived from skin keratinocytes and have mutant type p53 gene, showed that Axin1 overexpression and AKI treatment induced caspase-3 activation and PARP cleavage (Supplementary Fig. S6). These results suggested that PARP mediated cell death of L-Axin cells is at least in part based on the specific features of L929 cells.

AKI treatment of L-Axin cells induced cell membrane rupture, which is a hallmark of necrotic cell death. This observation led us to

investigate PARP activity in AKI-treated cells because PARP is involved in necrosis as well as apoptosis [Koh et al., 2005; Heeres and Hergenrother, 2007; Wang et al., 2009]. PARP activity was significantly elevated in AKI-treated L-Axin cells and inhibition of PARP activity reduced cell death effects of AKI. Among PARPs belonging to a family of 17 members, PARP-1 is the most abundant member and thus, PARP-1 activation by AKI treatment was initially expected. However, in our results, PARP-1 Knockdown failed to suppress AKI induced cell death of L-Axin cells although PARP inhibitor suppressed efficiently. In addition, AKI-induced cell death was not suppressed by treatment of classical RARP inhibitor, 3-aminobenzamide. In literature, 5-iodo-6-amino-1,2-benzopyrone which was used in this study inhibits PARP activity, but appears to have distinct biochemical properties [Papeo et al., 2009]. For examples, 5-iodo-6-amino-1,2-benzopyrone protects peroxynitrite-induced cytotoxicity in addition to hydroxyl radicals. These results implicated AKI treatment of L-Axin cells might induce atypical PARP activation, suggesting that PARP other than PARP-1 might be involved in AKI-induced cell death.

Previously, direct interaction of Axin with tankyrase (PARP-5) was described [Huang et al., 2009]. Tankyrase PARylates both Axin1 and Axin2, which is followed by ubiquitination and proteosomal degradation. Therefore, tankyrase inhibitions using siRNA or chemical inhibitors stabilize both Axins. In our results, AKI treatment induced cell death in L-Axin cells more efficiently than in L-Axin2 cells. Considering tankyrase interacts both Axin-1 and Axin-2 [Huang et al., 2009], Axin stabilizing effect of tankyrase may not be involved in AKI-induced cytotoxicity under Axin over-expressing condition. Several tetracycline antibiotics, including doxycyclin, have inhibitory effects on PARP-1 activity [Alano et al., 2006]. Because our system used the same amount of doxycyclin for induction of Axin and GFP expression in all three cells, low levels of PARP activation in L-Axin2 cells might not have been due to the inhibitory effects of doxycyclin.

Several reports showed that PARP is required for the translocation of AIF from the mitochondria to the nucleus and that AIF is necessary for PARP-dependent cell death [Wang et al., 2009]. Cell death signals frequently induce mitochondrial AIF release together with cytochrome *c*, but AIF appeared to be released from the mitochondria by a mechanism distinct from that of cytochrome *c* [Cregan et al., 2002]. In an ischemia model of cortical neurons, a caspase-3 inhibitor (DEVD) suppressed oxygen/glucose deprivation-induced mitochondrial cytochrome *c* release, but AIF release was not affected [Singh et al., 2010]. Considering these observations, PARP activation in our system may only stimulate mitochondrial release of AIF.

Given that Axin1 is regarded as a concentration-limiting regulator for Wnt signaling, changes in Axin1 expression level may critically influence various Axin1-involved events. For example, studies have shown that retinoic acid (RA) inhibits glioma cell proliferation, which is accompanied by up-regulation of Axin1 expression and altered subcellular distribution of β-catenin [Lu et al., 2008], suggesting that RA induces the trans-repressing of Wnt signaling. In lung cancer specimens, Axin1 expression was significantly lower in non-small-cell lung cancer (NSCLC) tissues than in normal lung tissues, but X-radiation increased Axin1 expression in NSCLC tissues [Han et al., 2009]. Thus, an increase of Axin1 expression weakens cell proliferation and viability.

In conclusion, our results suggest that Axin1 expression facilitates cell death induced by mitotic defects, especially when Aurora kinase activity is suppressed.

ACKNOWLEDGMENTS

This work was supported by a KOSEF Grant (2009-0080582 to S.-H.K. and R21-2005-000-10017-02007 to K.-J.S.).

REFERENCES

Alano CC, Kauppinen TM, Valls AV, Swanson RA. 2006. Minocycline inhibits poly(ADP-ribose) polymerase-1 at nanomolar concentrations. Proc Natl Acad Sci USA 103:9685–9690.

Behrens J, Jerchow B-A, Wurtele M, Grimm J, Asbrand C, Wirtz R, Kuhl M, Wedlich D, Birchmeier W. 1998. Functional interaction of an axin homolog, conductin, with β-catenin, APC, and GSK3. Science 280:596–599.

Chia IV, Costantini F. 2005. Mouse Axin and Axin2/Conductin proteins are functionally equivalent *in vivo*. Mol Cell Biol 25:4371–4376.

Cregan SP, Fortin A, MacLaurin JG, Callaghan SM, Cecconi F, Yu S-W, Dawson TM, Dawson VL, Park DS, Kroemer G, Slack RS. 2002. Apoptosis-inducing factor is involved in the regulation of caspase-independent neuronal cell death. J Cell Biol 158:507–517.

Curry J, Angove H, Fazal L, Lyons J, Reule M, Thompson N, Wallis N. 2009. Aurora B kinase inhibition in mitosis: Strategies for optimising the use of aurora kinase inhibitors such as AT9283. Cell Cycle 8:1921–1929.

Ditchfield C, Johnson VL, Tighe A, Ellston R, Haworth C, Johnson T, Mortlock A, Keen N, Taylor SS. 2003. Aurora B couples chromosome alignment with anaphase by targeting BubR1, Mad2, and Cenp-E to kinetochores. J Cell Biol 161:267–280.

Dreier MR, Grabovich AZ, Katusin JD, Taylor WR. 2009. Short and long-term tumor cell responses to Aurora kinase inhibitors. Exp Cell Res 315:1085–1099.

Fu J, Bian M, Jiang Q, Zhang C. 2007. Roles of aurora kinases in mitosis and tumorigenesis. Mol Cancer Res 5:1–10.

Fumoto K, Kadono M, Izumi N, Kikuchi A. 2009. Axin localizes to the centrosome and is involved in microtubule nucleation. EMBO Rep 10:606–613.

Gao C, Chen Y-G. 2010. Dishevelled: The hub of Wnt signaling. Cell Signal 22:717–727.

Girdler F, Gascoigne KE, Eyers PA, Hartmuth S, Crafter C, Foote KM, Keen NJ, Taylor SS. 2006. Validating Aurora B as an anti-cancer drug target. J Cell Sci 119:3664–3675.

Gizatullin F, Yao Y, Kung V, Harding MW, Loda M, Shapiro GI. 2006. The Aurora kinase inhibitor VX-680 induces endoreduplication and apoptosis preferentially in cells with compromised p53-dependent postmitotic checkpoint function. Cancer Res 66:7668–7677.

Hadjihannas MV, Bruckner M, Jerchow B, Birchmeier W, Dietmaier W, Behrens J. 2006. Aberrant Wnt/β-catenin signaling can induce chromosomal instability in colon cancer. Proc Natl Acad Sci USA 103:10747–10752.

Hadjihannas MV, Bruckner M, Behrens J. 2010. Conductin/axin2 and Wnt signalling regulates centrosome cohesion. EMBO Rep 11:317–324.

Han Y, Wang Y, Xu H-T, Yang L-H, Wei Q, Liu Y, Zhang Y, Zhao Y, Dai S-D, Miao Y, Yu J-H, Zhang J-Y, Li G, Yuan X-M, Wang E-H. 2009. X-radiation induces non-small-cell lung cancer apoptosis by upregulation of Axin expression. Int J Radiat Oncol Biol Phys 75:518–526.

Harrington EA, Bebbington D, Moore J, Rasmussen RK, Ajose-Adeogun AO, Nakayama T, Graham JA, Demur C, Hercend T, Diu-Hercend A, Su M, Golec

JMC, Miller KM. 2004. VX-680, a potent and selective small-molecule inhibitor of the Aurora kinases, suppresses tumor growth in vivo. Nat Med 10:262–267.

Heeres JT, Hergenrother PJ. 2007. Poly(ADP-ribose) makes a date with death. Curr Opin Chem Biol 11:644–653.

Hoar K, Chakravarty A, Rabino C, Wysong D, Bowman D, Roy N, Ecsedy JA. 2007. MLN8054, a small-molecule inhibitor of Aurora A, causes spindle pole and chromosome congression defects leading to aneuploidy. Mol Cell Biol 27:4513–4525.

Huang S-MA, Mishina YM, Liu S, Cheung A, Stegmeier F, Michaud GA, Charlat O, Wiellette E, Zhang Y, Wiessner S, Hild M, Shi X, Wilson CJ, Mickanin C, Myer V, Fazal A, Tomlinson R, Serluca F, Shao W, Cheng H, Shultz M, Rau C, Schirle M, Schlegl J, Ghidelli S, Fawell S, Lu C, Curtis D, Kirschner MW, Lengauer C, Finan PM, Tallarico JA, Bouwmeester T, Porter JA, Bauer A, Cong F. 2009. Tankyrase inhibition stabilizes axin and antagonizes Wnt signalling. Nature 461:614–620.

Itoh K, Krupnik VE, Sokol SY. 1998. Axis determination in Xenopus involves biochemical interactions of axin, glycogen synthase kinase 3 and β-catenin. Curr Biol 8:591–594.

Jeon SH, Yoon J-Y, Park Y-N, Jeong W-J, Kim S, Jho E-H, Surh Y-J, Choi K-Y. 2007. Axin inhibits extracellular signal-regulated kinase pathway by Ras degradation via β-catenin. J Biol Chem 282:14482–14492.

Katayama H, Sasai K, Kawai H, Yuan Z-M, Bondaruk J, Suzuki F, Fujii S, Arlinghaus RB, Czerniak BA, Sen S, 2004. Phosphorylation by aurora kinase A induces Mdm2-mediated destabilization and inhibition of p53. Nat Genet 36:55–62.

Kim S-M, Choi E-J, Song K-J, Kim S, Seo E, Jho E-H, Kee S-H. 2009. Axin localizes to mitotic spindles and centrosomes in mitotic cells. Exp Cell Res 315:943–954.

Koh DW, Dawson TM, Dawson VL. 2005. Mediation of cell death by poly(ADP-ribose) polymerase-1. Pharmacol Res 52:5–14.

Kojima K, Konopleva M, Tsao T, Nakakuma H, Andreeff M. 2008. Concomitant inhibition of Mdm2-p53 interaction and Aurora kinases activates the p53-dependent postmitotic checkpoints and synergistically induces p53-mediated mitochondrial apoptosis along with reduced endoreduplication in acute myelogenous leukemia. Blood 112:2886–2895.

Leung JY, Kolligs FT, Wu R, Zhai Y, Kuick R, Hanash S, Cho KR, Fearon ER. 2002. Activation of AXIN2 expression by β-catenin-T cell factor. J Biol Chem 277:21657–21665.

Li JJ, Li SA. 2006. Mitotic kinases: The key to duplication, segregation, and cytokinesis errors, chromosomal instability, and oncogenesis. Pharmacol Ther 111:974–984.

Li Q, Wang X, Wu X, Rui Y, Liu W, Wang J, Wang X, Liou Y-C, Ye Z, Lin S-C. 2007. Daxx cooperates with the Axin/HIPK2/p53 complex to induce cell death. Cancer Res 67:66–74.

Li Q, Lin S, Wang X, Lian G, Lu Z, Guo H, Ruan K, Wang Y, Ye Z, Han J, Lin S. 2009. Axin determines cell fate by controlling the p53 activation threshold after DNA damage. Nat Cell Biol 11:1128–1134.

Li M, Jung A, Ganswindt U, Marini P, Friedl A, Daniel PT, Lauber K, Jendrossek V, Belka C. 2010. Aurora kinase inhibitor ZM447439 induces apoptosis via mitochondrial pathways. Biochem Pharmacol 79:122–129.

Los M, Mozoluk M, Ferrari D, Stepczynska A, Stroh C, Renz A, Herceg Z, Wang Z-Q. Schulze-Osthoff K. 2002. Activation and caspase-mediated inhibition of PARP: A molecular switch between fibroblast necrosis and apoptosis in death receptor signaling. Mol Biol Cell 13:978–988.

Lu J, Zhang F, Zhao D, Hong L, Min J, Zhang L, Li F, Yan Y, Li H, Ma Y, Li Q. 2008. ATRA-inhibited proliferation in glioma cells is associated with subcellular redistribution of beta-catenin via up-regulation of Axin. J Neurooncol 87:271–277.

Margolis RL, Lohez OD, Andreassen PR. 2003. G1 tetraploidy checkpoint and the suppression of tumorigenesis. J Cell Biochem 88:673–683.

Neo SY, Zhang Y, Yaw LP, Li P, Lin S-C. 2000. Axin-induced apoptosis depends on the extent of its JNK activation and its ability to down-regulate [beta]-catenin levels. Biochem Biophys Res Commun 272:144–150.

Papeo G, Forte B, Orsini P, Perrera C, Posteri H, Scolaro A, Montagnoli A. 2009. Poly(ADP-ribose) polymerase inhibition in cancer therapy: Are we close to maturity? Expert Opin Ther Pat 19:1377–1400.

Sakanaka C, Weiss JB, Williams LT. 1998. Bridging of β-catenin and glycogen synthase kinase-3β by Axin and inhibition of β-catenin-mediated transcription. Proc Natl Acad Sci USA 95:3020–3023.

Salahshor S, Woodgett JR. 2005. The links between axin and carcinogenesis. J Clin Pathol 58:225–236.

Singh MH, Brooke SM, Zemlyak I, Sapolsky RM. 2010. Evidence for caspase effects on release of cytochrome c and AIF in a model of ischemia in cortical neurons. Neurosci Lett 469:179–183.

Tarnawski A, Pai R, Chiou SK, Chai J, Chu EC. 2005. Rebamipide inhibits gastric cancer growth by targeting survivin and Aurora-B. Biochem Biophys Res Commun 334:207–212.

Tong T, Zhong Y, Kong J, Dong L, Song Y, Fu M, Liu Z, Wang M, Guo L, Lu S, Wu M, Zhan Q. 2004. Overexpression of Aurora-A contributes to malignant development of human esophageal squamous cell carcinoma. Clin Cancer Res 10:7304–7310.

Vercammen D, Beyaert R, Denecker G, Goossens V, Van Loo G, Declercq W, Grooten J, Fiers W, Vandenabeele P. 1998a. Inhibition of caspases increases the sensitivity of L929cells to necrosis mediated by tumor necrosis factor. J Exp Med 187:1477–1485.

Vercammen D, Brouckaert G, Denecker G, Van de Craen M, Declercq W, Fiers W, Vandenabeele P. 1998b. Dual signaling of the Fas receptor: Initiation of both apoptotic and necrotic cell death pathways. J Exp Med 188:919–930.

Vischioni B, Oudejans JJ, Vos W, Rodriguez JA, Giaccone G. 2006. Frequent overexpression of aurora B kinase, a novel drug target, in non-small cell lung carcinoma patients. Mol Cancer Ther 5:2905–2913.

Wang Y, Dawson VL, Dawson TM. 2009. Poly(ADP-ribose) signals to mitochondrial AIF: A key event in parthanatos. Exp Neurol 218:193–202.

Willert K, Shibamoto S, Nusse R. 1999. Wnt-induced dephosphorylation of Axin releases β-catenin from the Axin complex. Genes Dev 13:1768–1773.

Yamamoto H, Kishida S, Uochi T, Ikeda S, Koyama S, Asashima M, Kikuchi A. 1998. Axil, a member of the Axin family, interacts with both glycogen synthase kinase 3β and β-catenin and inhibits axis formation of Xenopus embryos. Mol Cell Biol 18:2867–2875.

Yang H, Burke T, Dempsey J, Diaz B, Collins E, Toth J, Beckmann R, Ye X. 2005. Mitotic requirement for aurora A kinase is bypassed in the absence of aurora B kinase. FEBS Lett 579:3385–3391.

Zeng L, Fagotto F, Zhang T, Hsu W, Vasicek TJ, Perry WL, Lee JJ, Tilghman SM, Gumbiner BM, Costantini F. 1997. The mouse fused locus encodes Axin, an inhibitor of the Wnt signaling pathway that regulates embryonic axis formation. Cell 90:181–192.

Zhang D, Hirota T, Marumoto T, Shimizu M, Kunitoku N, Sasayama T, Arima Y, Feng L, Suzuki M, Takeya M, Saya H. 2004. Cre-loxP-controlled periodic Aurora-A overexpression induces mitotic abnormalities and hyperplasia in mammary glands of mouse models. Oncogene 23:8720–8730.